Power Cable Design and Dynamic Analysis for a Hybrid Platform

Sung Youn Boo
VL Offshore LLC
Houston, Texas, USA

He Yang
Ocean Engineering Department, Texas A&M University
College Station, Texas, USA

ABSTRACT

A semi-submersible hybrid platform moored at a water depth of 80 m is designed to generate a total of 10 MW power combining winds and waves. A power cable transferring the generated power connected to the platform is deployed in the water with a lazy-wave shape configuration. Two different length of the cables are considered to assess the cable performances under the design loading conditions of power production, extreme and survival storm conditions. A fully coupled dynamic analyses are carried out in time domain so that the cable responses induced by the coupled effects from the platform, mooring and cable are evaluated. Strength of the cables is assessed with respect to the tension loads, hang-off load angles and minimum bend radius along the cable length. The cable strength is validated with the design criteria. Fatigue damages of the cables are also simulated by implementing site scatter diagram. It is confirmed that the minimum fatigue life estimated is sufficiently longer than the allowable minimum.

KEY WORDS: Power cable; dynamic performance; fatigue analysis; offshore hybrid platform; semi-submersible

INTRODUCTION

Great efforts have been devoted to harvest the ocean renewable energies over the past decades. There are advantages of the renewable energies in many aspects, including sustainability and cleanliness, over the traditional fossil fuel. In order to design a floating offshore energy farm producing wind, wave or hybrid energy, a power cable transferring the generated power under a variety of sea environments plays an important role to ensure the integrity and safety of the power generating system, in addition to the design of the platform hull, mooring and installation.

There have been studies in the power cable using numerical and experimental methods. Martinelli et al. (2010) compared the numerical and experimental results of a lazy wave power cable. Prat (2011) studied the power cable performances with a catenary configuration at a shallow water depth, considering the cable end conditions. Fatigue evaluations were carried on the cable copper conductors or marine umbilical cable by several authors; Nasution (2014), Karlsen et al. (200), Thies et al. (2012) and Balena and Williams (2009).

In the present study, strength and fatigue performances of subsea dynamic power cable transferring the power generated from a hybrid platform are assessed. The hybrid platform is a semisubmersible type designed to generate a 10MW power combining wind and wave energies. The platform is moored with eight mooring lines at a water depth of 80 m off the coast of South Korea. The subsea power cable is connected to the middle of the platform pontoon keel and configured as a lazy-wave. Details of the platform responses can be found in Boo et. al (2016). Conceptual design results are also summarized in Kim et al. (2015).

Two different length power cables with 520 m and 180 m are considered separately in the present study. The cable configuration is optimized by iterations to minimize the impact to the hang-off tensions and curvature along the cable. The cable end on the seabed is assumed anchored. To minimize the excessive bending load near anchor of the cable of 180 m, a measure is introduced to the end section of the cable, which is similar to a bend stiffener.

The cable strength is simulated for the design sea states including operating (power production), extreme and survival conditions. In addition, one loading case of extreme sea states with one mooring line damaged is also simulated and analyzed. Global strength is assessed with respect to the tension loads and load angles at the cable hang-off, as well as the Minimum Bend Radius (MBR) along the cable length. All the simulated values in time domain are evaluated with Weibull extreme methods. Static and dynamic MBRs are also investigated against the allowable design criteria.

Long term fatigue performance is computed with site scatter diagram. Strains along the entire cable which are induced by each fatigue bin's wind, wave and current are simulated in time domain. Strain and cycles are estimated by Rainflow counting method. Damage to the cable is then evaluated utilizing a strain-cycles curve of copper.

In the following sections, the cable design conditions, Metocean data,

cable and platform configurations, cable strength and fatigue analyses are described.

CABLE DESIGN CONDITIONS

Metocean Conditions

The site specific metocean conditions are used for the hybrid platform design and dynamic cable analysis. Table 1 summarizes the metocean conditions for the Design Loading Cases (DLCs), including production (or operating) (PO), extreme (EX) and survival (SV) cases. A 50-year extreme condition is used based on ABS (2013), but 100-year condition is used as a survival condition. It is assumed that the winds, waves and currents are co-directional (COD). The current velocity profiles are estimated using a 1/7 power law.

Table 1. Metocean condition

Design Loading Case	Operating	Extreme	Survival
Environmental direction	COD	COD	COD
Wave	10-yr	50-yr	100-yr
Hs (m/s)	7.67	9.72	11.32
Tp (s)	12.4	13.98	15.1
Gamma	2.2	3	3
Wind 1hr Ave @ 10m (m/s)	13	41.24	45.99
Current Velocity (m/s)	1.27	1.14	1.22

Cable Design

Power cable strength and fatigue is designed to comply with the requirements in API RP 2RD (2009), API SPEC (2017) or ISO (2009).

PLATFORM CONFIGURATION

The semi-submersible hybrid platform with 10 MW power rate consists of the platform hull, mooring lines, power cable, wind turbines, wave energy converters (WECs) and other equipment. Fig. 1 illustrates the hybrid platform configuration presenting the major components. Key parameters of the platform are summarized in Table 2.

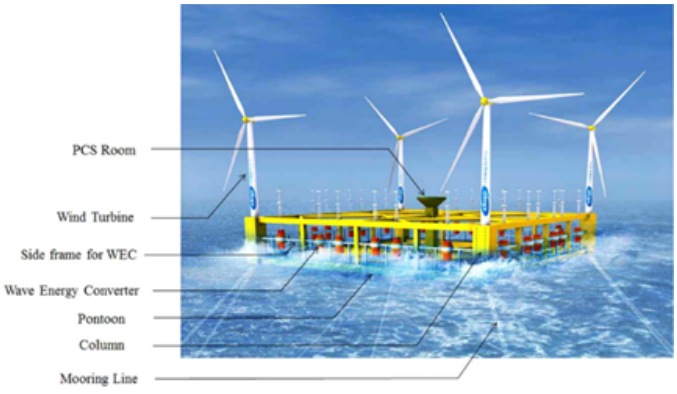

Fig. 1 10MW Hybrid semi-submersible platform configuration

The platform is moored with a total of eight chain lines with a group of two. Each mooring line is 500 m long including six clumps attached to the line on the seabed. The chain is a R4 studless chain with 157 mm diameter.

Table 2. Key parameters of 10 MW hybrid platform

Descriptions	Unit	Value
Displacement	ton	27,266
Draft	m	15.0
KG	m	15.35
Natural period: surge/sway	s	183.73
heave	s	16.63
roll/pitch	s	16.15
yaw	s	183.53
Mooring lines (groups)	-	8 (4)
length each	m	500

POWER CABLE CONFIGURATION

There are several options for the power cable installation, depending on water depth, platform type, cable hang-off tension, cable bend radius and cable fatigue near touch-down zone. For the present study, a lazy wave configuration is chosen for the cable, to minimize the loads induced by the dynamic couples between the platform and cable. Fig 2 shows a layout of the power cable together with eight mooring lines. The power cable is laid running toward the platform east (0 deg direction). All the mooring lines are numbered clockwise, starting from those two at the northeast group.

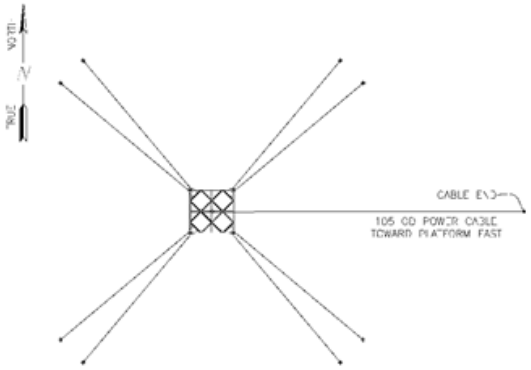

Fig. 2 Power cable layout with mooring system (plan view)

The power cable properties are summarized in Table 3. The lazy wave shape of the cable is configured with a total of 25 buoyancy modules. The modules with a length and diameter of 0.45 m are distributed with 1.0 m interval and start at 84 m from the hang-off point.

Table 3. Power cable properties

Parameters	Units	Values
Outside diameter	mm	105
Weight in air	kg/m	21.5
Minimum Braking Load	kN	270
Static minimum bend radius	m	1.05
Dynamic minimum bend radius	m	1.575
Bending stiffness	Nm^2	3,473
Axial stiffness	MN	151.2
Torsional stiffness	kNm^2	10

NUMERICAL MODELING

Turbine rotor is modeled as a disk producing the equivalent time-varying thrusts for the incident winds. Turbine thrusts on the upstream and downstream turbines are applied differently due to the wake effects to the downstream. The thrusts on the downstream turbines are derived using a method described in Boo et al. (2016) and applied accordingly to the down-stream turbine top. The present rotor modeling is similar to a semi-coupled scheme (ABS 2013), where the tower and platform coupled effects are neglected as the tower is included in a part of rigid hull of the platform, but the rotor thrusts are input every time step in time domain.

Fully coupled system is numerically modeled and simulated using OrcaFlex software. The power cable is modeled with multiple mesh segments. A finer mesh on the cable is typically required near the touch-down and the cable hang-off location (Jin and Kim, 2018). The cable top end is assumed to be connected to the center of the pontoon keel with a pinned condition at hang-off point. A perspective view of the modeled hybrid platform with the mooring lines and power cable is shown in Fig. 3.

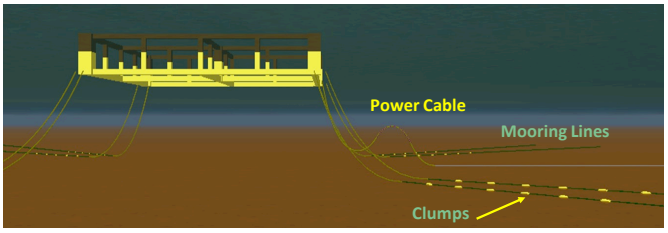

Fig. 3 Hybrid platform, mooring lines and power cable

The location and distribution of the buoyancy modules described earlier are the optimized final results for the lazy-wave shape considering the cable tension, minimum bend radius, cable submergence, platform offset (excursion), and starting locations of the buoyancy modules. These results lead to the buoyancy module starting at the location of 84 m.

The nonlinear wave loading is simulated with JONSWAP spectrum using the parameters in Table 1. The wind loadings on both hull and wind turbine tower are estimated based on the ABS FPI (2013) and input as wind load coefficients. As to the current loading, the underwater structures of the hybrid platform, mooring lines and power cables are modeled with drag coefficients. The platform hull viscous damping is also implemented by Morrison drag coefficients.

The fully coupled nonlinear response analysis is carried out in time domain excluding the ramp time. Maximum or minim values of the responses are estimated with a Weibull extreme method, based on three hours simulation.

NUMERICAL RESULTS AND DISCUSSIONS

Cable Static Tension Analysis

Static analysis for the power cable with mooring intact conditions is first conducted for the case with no external loadings prior to the dynamic cable analysis. Factor of Safety (FoS) of the hang-off tension for the 520 m cable is 33 and the Minimum Bend Radius (MBR) is about 85×OD at 98.78 m arc length from the hang-off end. Similar results are obtained for the 180 m cable. It is confirmed that both static tension FoSs and MBRs are far greater than the allowable design limits in Table 3.

Cable Dynamic Tension Analysis

The three types of loading cases of power production, extreme and survival cases, are simulated for three environmental directions, causing the platform offsets toward the cable laid (called near, 0 deg), cross (90 deg or 270 deg), outward (far, 180 deg) directions. A total of nine load cases with mooring line intact case are analyzed. In addition, three more cases with one mooring line damage are taken into consideration for the extreme events. The damaged lines of ML#2, 5 and 6 are selected from the mooring analysis such that these lines are the most loaded lines associated with the environment headings of 0, 90 and 180 deg, respectively.

Table 4 and Table 5 summarize the dynamic tensions of mean, Standard Deviation (STD), maximum and FoS at the cable hang-off for the intact and damaged cables under the various loading conditions. In the course of the present study, Weibull, Rayleigh and generalized Pareto extreme methods are utilized to compute the maximum, but Weibull extreme values are presented in this paper. It is seen that all the maximum tensions at the hang-off point are under the safe criteria for the power cable. Overall, the far conditions cause the low FoS due to the taut cable line created by the platform offset. The lowest FoS is occurred for the #ML 2 damage with 180 deg heading (far case). Overall performances of both cable lengths to the tensions are observed to be similar to each other.

Table 4. Dynamic tensions at cable hang-off for 520 m power cable

DLCs	Mooring	Head. (deg)	Mean (kN)	STD (kN)	Max. (kN)	FoS
PO	Intact	0	7.86	0.31	9.20	29.34
		90	9.28	0.25	10.22	26.41
		180	10.51	1.24	22.09	12.22
EX	Intact	0	7.81	0.35	9.17	29.45
		90	10.01	1.23	15.26	17.70
		180	11.14	2.98	57.85	4.67
	#6 damage	0	7.80	0.35	8.86	30.47
	#5 damage	90	10.20	0.98	15.45	17.47
	#2 damage	180	12.45	4.76	71.57	3.77
SV	Intact	0	7.89	0.47	10.35	26.09
		90	16.21	4.23	36.37	7.42
		180	12.38	5.41	90.55	2.98

Table 5. Dynamic tension at cable hang-off for 180 m power cable

DLCs	Mooring	Head. (deg)	Mean (kN)	STD (kN)	Max. (kN)	FoS
PO	Intact	0	7.89	0.32	9.31	29.01
		90	9.46	0.22	10.35	26.09
		180	11.42	1.93	31.40	8.60
EX	Intact	0	7.82	0.35	9.18	29.42
		90	9.20	0.21	10.24	26.38
		180	12.59	4.75	88.37	3.06
	#6 damage	0	7.81	0.35	8.91	30.32
	#5 damage	90	8.99	0.20	9.94	27.17
	#2 damage	180	14.91	8.33	138.0	1.96
SV	Intact	0	7.89	0.47	10.40	25.97
		90	9.50	0.33	11.59	23.29
		180	14.37	8.34	129.7	2.08

Cable Minimum Bend Radius Analysis

In addition to the tension, the minimum bend radius is another key performance subject of a power cable design. Small bend radius against the allowable minimum given by cable suppliers may cause damage to the cable, especially under a periodic stress and strain. Thus, the dynamic MBRs are set higher than the static MBRs as shown in Table 3. Statistical analysis results of the MBRs of the dynamic cables for all the cases are listed in Table 6 and Table 7, respectively, for two different power cable length options. Here, each location of the lowest MBR along the cable arc length from the hang-off is presented in the 4th column of each Table.

Table 6. Dynamic minimum bend radius for 520 m power cable

DLCs	Mooring	Head. (deg)	Locat. (m)	Mean (m)	STD (m)	MBR (m)
PO	Intact	0	161.75	2.54	0.70	2.32
		90	91.42	20.05	0.98	16.33
		180	88.52	24.83	7.47	11.10
EX	Intact	0	160.75	3.11	1.02	2.37
		90	92.87	24.58	6.41	14.18
		180	87.18	28.15	15.63	10.18
	#6 damage	0	162.75	2.68	0.01	2.59
	#5 damage	90	92.87	26.10	4.76	15.53
	#2 damage	180	87.18	34.77	26.93	11.55
SV	Intact	0	168.75	4.53	5.37	2.73
		90	88.63	48.70	14.90	14.98
		180	85.73	34.88	39.48	9.58

Table 7. Dynamic minimum bend radius for 180 m power cable

DLCs	Mooring	Head. (deg)	Locat. (m)	Mean (m)	STD (m)	MBR (m)
PO	Intact	0	160.50	2.52	0.58	2.35
		90	171.95	2.02	0.05	1.99
		180	88.52	29.65	10.10	12.10
EX	Intact	0	156.50	4.69	0.81	2.38
		90	171.95	1.80	0.10	1.72
		180	87.07	35.39	26.81	10.42
	#6 damage	0	162.50	2.41	0.05	2.32
	#5 damage	90	171.95	1.75	0.01	1.69
	#2 damage	180	171.95	196.1	349.6	10.99
SV	Intact	0	166.50	3.37	8.41	1.78
		90	171.95	1.69	0.06	1.59
		180	87.07	55.63	817.0	8.27

The resulting MBRs for both cable options of 520 and 180 m are greater than the allowable minimum of 1.575 m (Table 3), indicating that either option will be a workable option for the present platform. But the shorter cable meets the criteria marginally for the cross case under survival condition, which is due to higher bending load near the cable end termination.

The lowest MBR locations of the 520 m cable move toward the hang-off end when the headings change from 0 to 180 deg. However, the range of this location is relatively stable, which is around 80 m to 170 m for the production, extreme and survival conditions. For the 180 m cable, the lowest MBR locations occur for the cross cases and are very close to the cable end termination anchored. As described above, the higher bending loads near the end termination cause the lower MBR as depicted in Fig 4. The large cable displacement due to the environmental loads deforms the cable curvature significantly near the cable end. A care is, thus, recommended to design the cable end segment for the cable of 180 m or shorter.

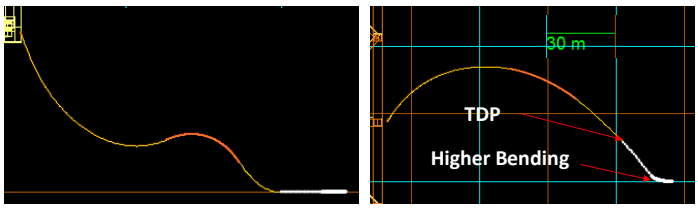

Fig. 4 Dynamic profiles of power cable of 180 m for cross case (elevation and plan view)

Hang-off Tension and Angle Analysis

The submerged weight of vertically suspended cable on stationary or floating platforms is carried by hang-off. A bend stiffener tied to the platform is typically used at the hang-off section of the cable, but a pin-joint condition is applied at the hang-off instead of modeling the bend stiffener, as we focus on the relationships between the end loads (hang-off tensions) and the associated load-angles for a future bend stiffener design.

The hang-off end acts as the connection point between platform and the power cable. Thus, the cable hang-off loads are strongly coupled with the platform responses which may have non-linear components. In order to carry out the spectral analysis of the end loads, the 180 m long cable is selected. Fig. 5 compares the spectra of the extreme and survival end loads for the far case (180 deg). The first peak at the lowest frequency indicates the hang-off end coupling effect with the platform's surge motion. The second peak is associated with the wave spectra peak frequency (Table 1). The third and fourth peaks are higher harmonics of the wave frequency. Strong non-linear effects on the end loads due to the waves are observed, especially in the survival condition.

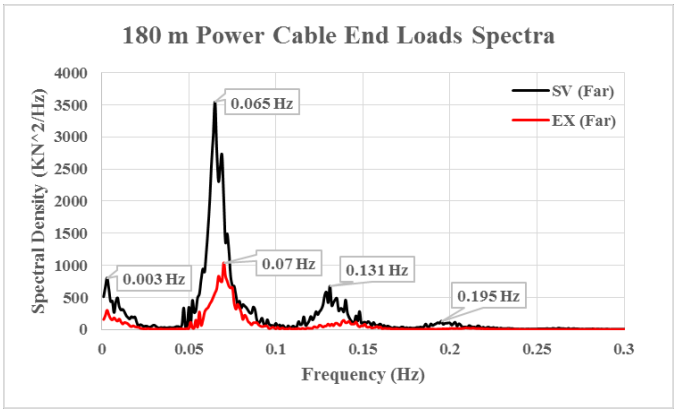

Fig. 5 End loads spectra for 180 m power cable

To demonstrate the relationship between the cable end load and its angle at the hang-off, the extreme and survival conditions are also selected and the instantaneous loads vs. angles are shown in Fig. 6 and Fig. 7. Here, the direction of the end load is along the tangential of the cable at hang-off point, while the load angle is defined as the angle between the end load vector and the pre-set cable axial direction of the fitting which is set as 174 deg for the present study as illustrated in Fig. 8. A pinned condition at hang-off point is undertaken as described.

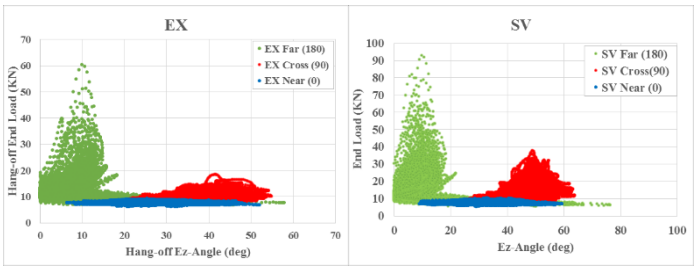

Fig. 6 End load and angle at hang-off for 520 m power cable

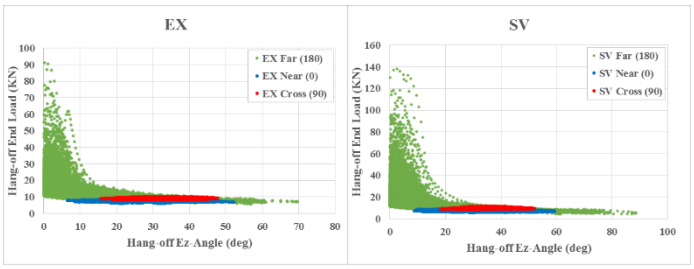

Fig. 7 End load and angle at hang-off for 180 m power cable

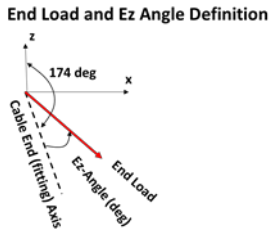

Fig. 8 End load and Ez angle definition

The majority of the load angles for the extreme and survival far cases fall within the range of 20 deg, indicating the cable near the hang-off becomes more taut line shape with higher tension loads. Higher angles for the far case are presented with the very small end loads, which is mainly due to the relative platform pitch causing the cable top segments to be pulled downward instantly but the next segments to be buoyant by opposite phase action creating very small load on the cable. It is also observed that the shorter line of 180 m under the cross and near conditions has a narrower tension band compared to the 520 m cable.

Cable Touch-Down Point Analysis

Touch-Down Points (TDPs) of the dynamic cable vary with the platform motions associated with the environment conditions. In Fig. 9 and Fig. 10, are compared the distributions of the cable TDPs for the four different loading cases of production (operating), extreme, extreme with one line damaged and survival.

For the 90 deg cross case, the TDPs of the 520 m cable spread very widely compared to the 180 m cable which has rather concentrated distribution. The TDPs spread in large ranges as the sea states increases to the extreme and survival seas. The 520 m cable has long seabed length so that it can be displaced transversely or longitudinally more easily than the 180 m cable, although there is a seabed friction against the cable displacements. For the 0 and 180 deg headings, the cable is laid such that TDP footprints are narrowly distributed along those directions.

In case of the cable of 180 m, all the cases have very similar distribution patterns of TDPs (Fig. 10). Especially for the cross headings, the TDPs are distributed within almost same ranges.

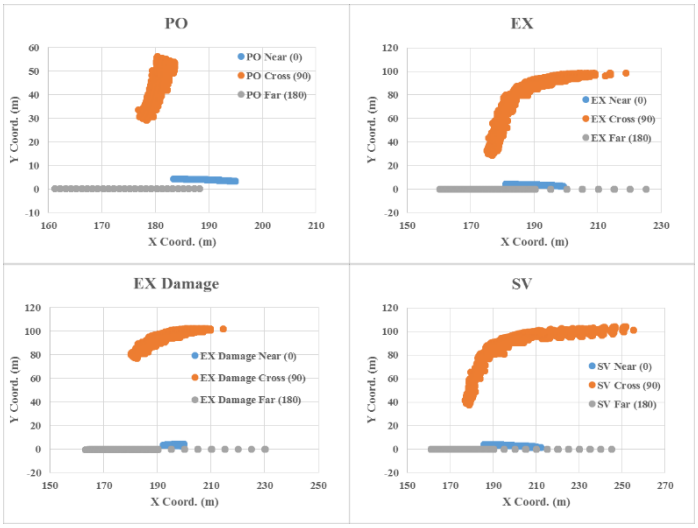

Fig. 9 Touch-down point distribution for 520 m power cable

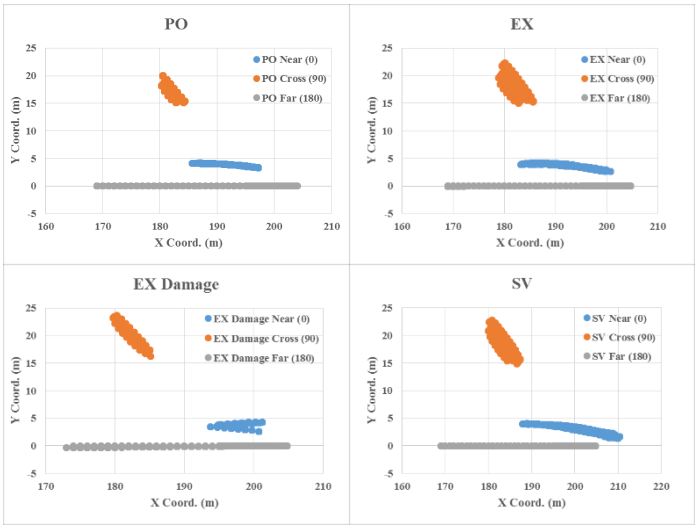

Fig. 10 Touch-down point distribution for 180 m power cable

Cable Fatigue Analysis

Fatigue strength design is another important subject for the cable design to prevent the fatigue failure. The design life of power cable and its components is 25 years. The minimum fatigue FoS of the cable considered is 10.

Power cable fatigue analysis is carried out with the condensed site scatter diagram consisting of 50 fatigue bins. The first 25 bins are associated with waves from NNW direction and the rest of them are from SSW. Fig. 11 shows the probability of each fatigue bin. The winds and currents are co-directional to the waves.

The dynamic analyses are run for all the bins using Orcaflex and the strain-cycle histograms are obtained using Rainflow counting method as described below. The strain-cycle (ε-N) curve (Karlsen et al., 2009) used for the fatigue damage evaluation is presented in Fig. 12.

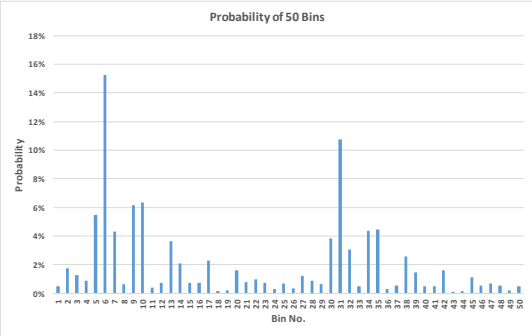

Fig. 11 Probability of fatigue bins

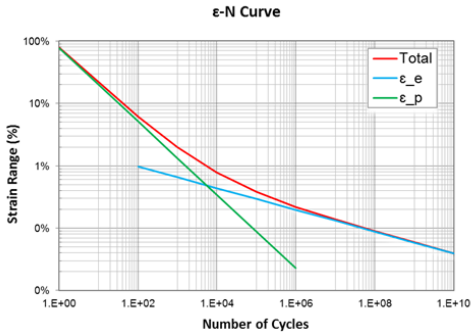

Fig. 12 Strain-cycle (ε-N) curve of copper conductor

The total strain amplitude (ε_a) is the sum of the elastic (ε_e) and the plastic (ε_p) strains and can be written as:

$$\varepsilon_{a,\ total} = \varepsilon_e + \varepsilon_p = C_e N^{-\beta_e} + C_p N^{-\beta_p}$$

where C and β are material-dependent constants that describe the shape of the fatigue curve. The curve parameters of C and β are:

C_e=0.0219, β_e=0.1745; C_p=0.7692, β_p=0.5879

For the fatigue analysis, the power cable is divided into fine mesh segments. And on each segment, 16 angles along the peripheral direction are considered to calculate their corresponding damages over the total exposure time, among which the maximum one will be kept as the damage value for this segment. The final damage on each segment is, thus, the maxima among the damages corresponding to 16 angles.

A representative fatigue damages due to the bins are plotted in Fig. 13. The bin numbers 5 and 31 cause the dominant damages to the cable at the location, which is related to the higher probabilities of both bins as shown in Fig. 11.

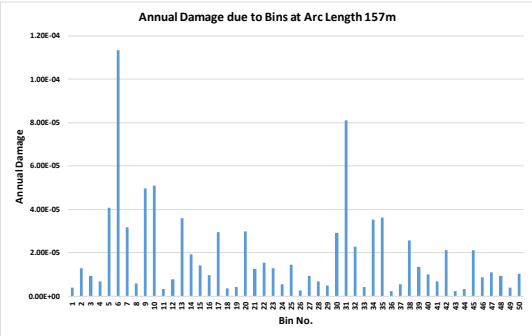

Fig 13 Annual damage due to bins on the 180 m cable

Fig. 14 shows the resulting fatigue life along the arc length of the power cable for 180 m power cable. Here, the static cable profile is also plotted for a reference. There are several low peaks on the curve which are located around the hang-off, buoyancy modules (point #1) and touch-down segments (point #2 and point #3). The points #1, #2 and #3 are located about 100 m arc length from the hang-off, 148 m and 157 m, respectively.

The fatigue analysis results suggest that the most probable damages occur around the cable touch-down segments, which is a typical result observed in other subsea umbilical designs. There might be some fatigue issues around the cable end termination which is currently modeled with a structure similar to a bend stiffener. Care is suggested at the end termination design in the future phase of work. Among those locations identified, the least life (or worst damage) is seen to be at the point #3 located beyond the static touch-down segment.

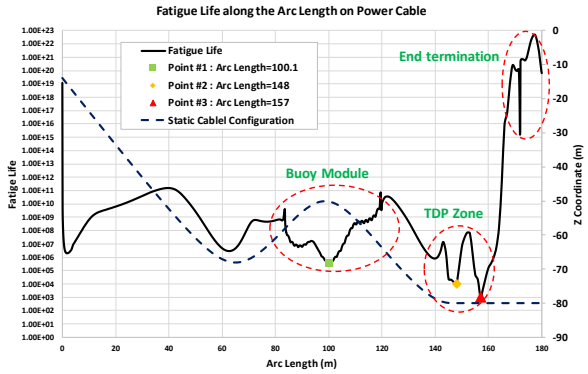

Fig. 14 Power cable fatigue life along the arc length for 180 m power cable

The least fatigue life estimated at point #3 (157 m from the hang-off) is 1,076 years and its fatigue FoS is about 43 which is much greater than the required minimum of 10. This confirms that the power cable design complies with the fatigue design criteria. The fatigue life of the 520 m cable is also estimated to be longer than the 180 m cable so that the details are not presented in this paper.

CONCLUSIONS

The present study focuses on a series dynamic simulations for the strength and fatigue design validation of a power cable which will be used for transferring the power of 10 MW generated from a hybrid semi-submersible platform. The platform is moored at a water depth of 80 m. Two cable length options of 180 m and 520 m are considered to assess the performances. The cable is connected to the platform keel and configured as a lazy-wave shape through an optimization of the buoyancy modules.

For the cable strength performance assessments, the cable tension, minimum bend radius, end load at hang-off together with the angle and touch-down point distribution are simulated using a fully coupled analysis considering the various design load cases of the power production, extreme, and survival conditions. It is verified that both power cables satisfy with the strength design requirements. It is, however, observed that the 180 m cable has, better performance in terms of the low variations of the hang-off load angles and limiting the touch-down point footprints.

Fatigue analysis of the cable is conducted in time domain using the sea states presented with the site fatigue bins. The fatigue damages along the

cable are computed with the histograms from a Rainflow counting method and strain-cycle curve of copper conductor. It is observed that the worst damages occur around the dynamic touch-down segments on the cable. It is proved that the fatigue life of the power cable is sufficiently longer than the required minimum.

ACKNOWLEDGEMENTS

The present work is a result of the project "Development of the design technologies for a 10MW class wave-offshore wind hybrid power generation system" granted by the Ministry of Oceans and Fisheries, Korea. All support is gratefully acknowledged.

REFERENCES

ABS FPI (2013). ABS FPI Guide for Building and Classing Floating Production Installations.

ABS (2013) ABS Guide Floating Offshore Wind Turbine Installations.

API RP 2RD (2009). Recommended Practice for Design of Risers for Floating Production Systems and TLPs.

API SPEC (2017). 17E Specification for Subsea Umbilicals.

Balena, R. and Williams, P (2009). "Risk-Based Structural Analysis of Frade Umbilical Cables," *20th International Congress of Mechanical Engineering,* November.

Boo, SY, Kim, K-H, Lee, K, Park, S, Choi, J-S, Hong, K (2016). "Design Challenge of a Hybrid Platform with Multiple Wind Turbine and Wave Energy Converters," *Proc. 21st Offshore Symposium, Society of Naval Architects and Marine Engineers*, Houston.

ISO (2009). ISO-13628-5 Petroleum Natural Gas Industries – Design and Operation of Subsea Petroleum Production Systems – Part 5: Subsea Umbilicals.

Jin, C and Kim, M-H (2018). "Time-Domain Hydro-Elastic Analysis of a SFT (Submerged Floating Tunnel) with Mooring Lines under Extreme Wave and Seismic Excitations," *Applied Sciences*, 8, 2386.

Karlsen, S, Slora, R, Heide, K, Lund, S, Eggertsen, F, and Osborg, PA (2009). "Dynamic Deep Water Power Cables," *Proceedings of the 9th International Conference and Exhibition for Oil and gas resources development of the Russian Arctic and CIS continental shelf, RAO/CIS Offshore*, St Petersburg, pp. 194–203.

Kim, K-H, Lee, K, Sohn, JM, Park, S-W, Choi, J-S, Hong, K (2015). "Conceptual Design of 10MW Class Floating Wave-Offshore Wind Hybrid Power Generation System," *Proceedings of the Twenty-fifth International Ocean and Polar Engineering Conference.*

Martinelli, L, Lamberti, A*, Ruol, P, Ricci, P, Kirrane, P, Fenton, C and Johanning, L (2010). "*Power Umbilical for Ocean Renewable Energy Systems – Feasibility and Dynamic Response Analysis*," 3rd Intl Conference on Ocean Energy, 6.*

Nasution, F, Savik, S and Berge, S, (2014) *"*Experimental and Finite Element Analysis of Fatigue Strength for 300 mm^2 Copper Power Conductor," *Marine Structures, 39.*

Prat, J, del Rio, J and Arbos, A (2011). "Preliminary study of Moored Power Cables*," Oceans.*

Thies, PR, Johanning, L and Smith, GH (2012) "Assessing Mechanical Loading Regimes and Fatigue Life of Marine Power Cables in Marine Energy Applications," *Special Issue Proceedings of the Institution of Mechanical Engineers, Part O: Journal of Risk and Reliability*.